European Journal of Clinical Pharmacy
Print ISSN: 2385-409X **Online ISSN**: 3105-0409
Website: https://farmclin.com/

Original Research Article

Integrated Computational and Experimental Identification of Broad-Spectrum Natural Lead Compounds against Dengue Virus

Article History:

Name of Author:
Telugu Seetharam Deepak[1], Anisha Jain[2], Baburao Gaddala[3], Padmesh Medesety[4], Bhargav Shreevatsa K S[5], Chandan D[5], Chandrashekar Srinivasa[1], Gopinath S M[1*]

Affiliation:
[1]*Department of studies in Biotechnology, Davangere University, Shivagangothri, Davangere, Karnataka, India*
[2]*Department of Biotechnology, JSS Science and Technology University, Mysuru, Karnataka, India*
[3]*Department of Chemical Engineering, School of Studies of Engineering and Technology, Guru Ghasidas Vishwavidyalaya, A Central University, Koni, Bilaspur, Chhattisgarh-495009, India.*
[4]*Department of Chemical Engineering, V.S.B. Engineering College Karur Affiliated To Anna University, Tamil Nadu-639 111, India*
[5]*Department of Microbiology, JSS Academy of Higher Education & Research Mysuru, Karnataka, India.*

Corresponding Author:
Gopinath S M

Received: 28-09-2025
Revised: *05*-11-2025
Accepted: 24-11-2025
Published: 26-12-2025

This is an open access journal, and articles are distributed under the terms of the Creative Commons Attribution-Noncommercial-Share Alike 4.0 License, which allows others to remix, tweak, and build upon the work non-commercially, as long as appropriate credit is given and the new creations are licensed under the identical terms.

Abstract: The global burden of dengue virus persists due to the lack of targeted antivirals and vaccine limitations. This study finds multi-target inhibitors derived from natural phytocompounds that can both reduce oxidative stress caused by infection and interfere with the DENV life cycle. ***Methods***: MM/GBSA calculations and high-throughput virtual screening were used to screen a natural compound library against six DENV targets (Capsid, Membrane, Envelope, NS2B/NS3, NS5, and NS1). Molecular dynamics (MD) simulations were performed on top hits for 100 ns. MTT, PRNT, and CPE-based antiviral tests were used to validate lead compounds in vitro using Vero E6 cells. ***Results***: Five lead compounds demonstrated superior docking scores. The MM/GBSA binding free energy analysis and MD simulations revealed that compounds NP4 and NP5 consistently exhibited the most favourable binding affinities and stable trajectories. NP5 (Vitexin) was the most effective in vitro compared to the other lead compound, Diosmetin and standard, Quercetin. In HepG2 cells, both leads decreased ROS levels, demonstrating cytoprotective antioxidant action. ***Conclusion***: The integrated data from cytotoxicity, plaque reduction, and in vitro antiviral tests collectively demonstrate that NP5 outperforms both NP4 and quercetin, emerging as a highly promising lead compound for future anti-dengue interventions.

Keywords: Dengue Virus; Vitexin; Phytocompounds; Antiviral; Virtual screening

INTRODUCTION

Dengue is a virus that is transmitted by mosquitoes and is the primary cause of arthropod-borne viral diseases around the globe. Dengue virus (DENV), which is mostly spread by *Aedes aegypti* and *Aedes albopictus*, can cause a variety of illnesses, from self-limiting dengue fever to potentially fatal diseases including Dengue Hemorrhagic Fever (DHF) and Dengue Shock Syndrome (DSS). There are currently no specific FDA-approved antiviral drugs available for clinical use, and current vaccines have issues with efficacy across all four serotypes and the risk of

 © 2025 European Journal of Clinical Pharmacy; Volume: 7: Issue: 1| All Right Reserved

antibody-dependent enhancement, despite the high global burden of the virus and its increasing geographic expansion due to urbanization and climate change[1,2].

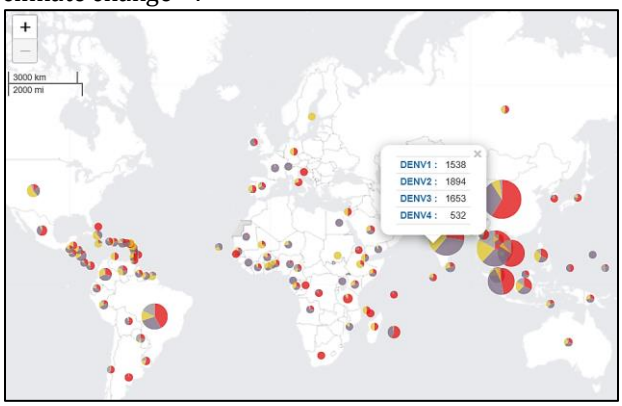

Figure 1. Global distribution of dengue virus serotypes (DENV1–4) based on WHO data (1960–2025). The pie charts represent the relative proportion of dengue virus serotypes across various geographic regions, highlighting the simultaneous circulation of multiple serotypes. (Source: World Health Organization (WHO). (2025). Global Dengue Surveillance: Genomic Data Dashboard. Retrieved June 27, 2025, from https://worldhealthorg.shinyapps.io/dengue_global/)[3]

The pie charts in **figure 1** represent the relative proportion of dengue virus serotypes across various geographic regions, highlighting the simultaneous circulation of multiple serotypes. DENV 1 accounts for the highest proportion (40.37%), followed by DENV2 (32.32%), DENV3 (18.10%), and DENV4 (9.20%). Co-circulation is most intense in Southeast Asia and South America, underscoring the risk of secondary infections and antibody-dependent enhancement (ADE). In India, DENV2 is the most prevalent (33.72%), followed by DENV3 (29.43%), DENV1 (27.38%), and DENV4 (9.47%)[3].

Dengue has become prevalent worldwide in both endemic and epidemic transmission patterns. The Indian subcontinent, because of its favorable environment, has numerous records of dengue outbreaks that involve all serotypes[2]. Although all major areas of the globe are impacted by rising dengue rates, around 75% of individuals infected with dengue reside in the Asia-Pacific region[4]. The World Health Organization identified dengue as one of the "top ten threats to global health in 2019". Dengue is present globally and appears endemically, sporadically, or as epidemics[5].

Seven non-structural proteins (NS1, NS2A, NS2B, NS3, NS4A, NS4B, and NS5) and three structural proteins (Capsid, Membrane, and Envelope) are encoded by the DENV genome. While non-structural proteins like the NS2B/NS3 protease and NS5 polymerase are crucial for RNA replication and polyprotein processing, respectively, structural proteins are necessary for viral assembly and entrance. The NS1 protein is also essential for vascular leakage and immune evasion. A viable approach to achieving broad-spectrum efficacy and lowering the risk of drug resistance is the development of therapies that can concurrently target several stages of this intricate viral life cycle[2,6]. Natural products have long been a rich supply of antiviral scaffolds with good safety profiles, especially secondary metabolites including flavonoids, alkaloids, and terpenoids. Many of these substances have innate anti-inflammatory and antioxidant qualities, which are essential for controlling the oxidative stress and cytokine storm linked to severe dengue. Since many of these compounds have polypharmacological actions that can disrupt both viral replication and host-mediated pathogenesis, using a library of natural products provides an advantageous starting point for drug discovery[7,8]. To find effective inhibitors against a panel of six crucial DENV targets-the capsid, membrane, envelope, NS2B/NS3 protease, NS5 polymerase, and NS1 protein, we used an integrated computational and experimental strategy in this investigation.

1. METHODS

1.1. Computational Screening of Phytocompounds

1.1.1. Pre-processing of the structures

The Schrödinger Suite 2022-3 version (Schrödinger, LLC, New York, NY, 2022) was used to conduct HTVS of the compound library of natural products (Cat. No.: HY-L021) acquired from the MedChemExpress (MCE)[9,10]. The three-dimensional structures of the most common and validated inhibitory targets of the DENV were taken from RCSB PDB database[11]. The structures of lead compounds were taken from the PubChem database. **Table 1** includes the proteins that were selected based on the literature and structural parameters. The pre-processing of the structures involved the assignment of bond orders, the addition of disulfide bonds and missing hydrogens, the use of the Prime module to fill in loop gaps, the removal of water molecules, ions, metals, and other co-crystallized ligands, and hydrogen bond optimization to optimize charge-charge interaction and hydrogen bonding via the Maestro workspace of the suite[9].

MCE offers a special assortment of the natural compounds, including flavonoids, alkaloids, quinones and terpenoids which are known to inhibit NS3 protease, NS5 polymerase, and envelope-mediated entry, making this library ideal for mechanistic screening. The drug library was prepared for HTVS using Schrödinger's LigPrep module. Using the force field OPLS_2005 (Optimized Potentials for Liquid Simulations), the energy of each pharmacological compound was minimized at pH 7.0 ± 2[9]. The

 © 2025 European Journal of Clinical Pharmacy; All Right Reserved

screened compounds were also compared with the list of antiviral phytocompounds from Dr. Duke's phytochemical and ethnobotanical database to filter molecules with antiviral biological activity[12].

Table 1. Dengue virus drug target proteins retrieved from the RCSB PDB.

Sl. No.	Molecule Name	PDB ID	Resolution	Three-dimensional structure
1.	Capsid premembrane protein[13]	6VG5	1.50 Å	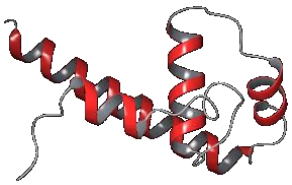
2.	Small membrane protein M[14]	3J2P	3.60 Å	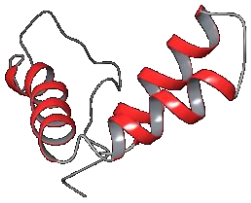
3.	Major envelope protein E[14]	3J2P	3.60 Å	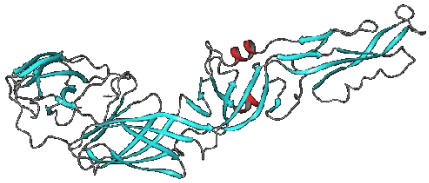
4.	NS2B/NS3 Protease[15]	2FOM	1.50 Å	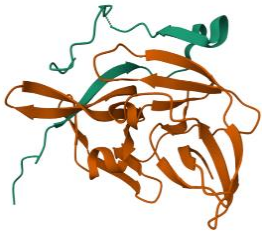
5.	Dengue 3 NS5 protein[16]	5JJR	1.99 Å	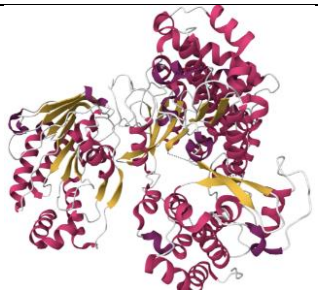

© 2025 European Journal of Clinical Pharmacy; All Right Reserved

6.	Dengue 2 NS1 protein[17]	4O6B	3.0	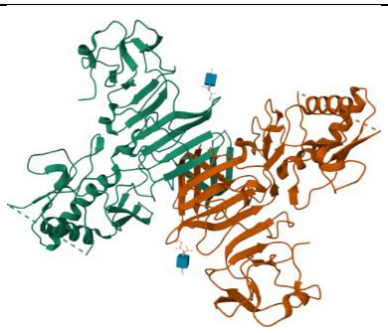

1.1.2. Binding site prediction and grid generation

Using Schrödinger Glide's receptor grid generation module, a grid surrounding the co-crystallized ligands was defined with a partial charge cut-off of 0.25 and a scaling factor of 1. Using Schrödinger Glide's SiteMap tool, the binding site residues for the protein which does not have a co-crystallized ligand were predicted[18,19].

1.1.3. HTVS of compound libraries against DENV structural proteins

Using the Schrödinger glide module, ligand-flexible docking was carried out using the HTVS precision mode and the SP (standard precision) mode using the standard inhibitors for comparison. Because glide docking approaches produce a docking score that is tied to the free energy of attaching a ligand to a receptor, the more negative the docking score, the better and larger the binding affinity[19,20].

1.1.4. MM/GBSA Free Energy of Binding Calculations

Molecular mechanics with generalised Born and surface area solvation (MM/GBSA) uses generalized Born (GB) and surface area (SA) terms to account for solvent effects. Further, this binding free energy (dGbind) calculation was also used to assess the strength of the inhibitor and the protein interaction as modelled. The following formula is used to calculate the binding-free energy of a protein and ligand:

$$\Delta G_{Bind} = \Delta G_{complex} - (\Delta G_{protein} + \Delta G_{ligand})$$

where $\Delta G_{protein}$ and ΔG_{ligand} are the free energies of the protein and ligand in the solvent, respectively, and ΔG_{Bind} is the total free energy of the complex. The prime module of the suite was used for these calculations using the OPLS4 force field and VSGB 2.0 solvation model. These analyses were done on all the top five hits against all the DENV target proteins[9,18-20].

1.1.5. Molecular Dynamics Simulation

The Desmond product of the Schrödinger suite was employed to perform the simulations for the docked complexes at 100 ns. The docked complexes were placed in an orthorhombic shaped box at a buffer distance of 16 Å solvated with SPC water model. To neutralize the systems, more Na+/Cl− ions were added and pressure and temperature were set at 1.01325 bar and 310 K, respectively[18-20]. The MD simulation trajectories were analyzed using simulation interaction diagram tool of Desmond module[9].

1.2. *In vitro* analysis of the top hit compounds

1.2.1. Chemicals and Reagents

The compounds screened via computational analyses were procured and purchased to evaluate the anti-dengue potential against viral cell lines. The compounds diosmetin (Cat No.: D7321) and vitexin (Cat No.: 49513) were purchased from Merck Sigma-Aldrich. All other chemicals and the reagents used were of analytical grade and purchased from Merck Sigma-Aldrich and Himedia, India. All the compounds were dissolved in DMSO, aliquoted to yield 50 mg/mL stocks and stored at -80ºC until further use.

1.2.2. Anti-inflammatory activity

For the ROS scavenging assay, HepG2 cells were seeded in 6-well plates at a density of 1×10^6 cells/well and treated with different concentrations of NP4 and NP5 compounds. The positive control group was exposed to 500 µM hydrogen peroxide (H_2O_2) for 1 hour to induce oxidative stress. Following treatment, cells were washed twice with PBS and incubated with 10 µM DCFH-DA (Dichlorofluorescin diacetate) for 30 minutes at 37°C. DCFH-DA is a non-fluorescent compound that, once inside the cells, is hydrolyzed to DCFH and then oxidized by ROS, resulting in the fluorescent DCF product. The fluorescence intensity of DCF was measured using a flow cytometer (BD FACSCalibur) at an excitation wavelength of 488 nm and emission at 525 nm. The percentage of cells showing fluorescence was used as an indicator of ROS levels in each group. Data were analyzed using FlowJo software, and the results were compared between the control, H_2O_2-treated, and NP4 and NP5-treated groups to assess the ROS scavenging activity of the compounds[21-23].

© 2025 European Journal of Clinical Pharmacy; All Right Reserved

1.2.3. Cytotoxicity Assay

To determine the non-toxic dose range of phytocompounds, the MTT assay was performed using Vero E6 cells that were seededat a density of 5 × 10^4 cells/well in 100 µL complete DMEM and incubated at 37°C for 24 hours[23]. Test compounds were added in serial dilutions ranging from 3.13 to 200 µg/mL. After treatment, 20 µL of 5 mg/mL 3-(4, 5-dimethyl-2-thiazolyl)-2, 5-diphenyl-2 H-tetrazolium bromide (MTT) solution was added to each well and incubated for 3 hours at 37°C. The formazan crystals formed were solubilized in 100 µL of DMSO, and absorbance was read at 570 nm and 490 nm using a microplate reader (Multiscan microplate spectrophotometer, Model No. 1530, Multisky, Thermo Fisher Scientific, USA). Quercetin was used as the positive control. Dose–response curves were constructed to determine CC_{50} (concentration reducing cell viability by 50%) and $MNTD_{80}$ (maximum non-toxic dose maintaining ≥80% viability) using nonlinear regression in GraphPad Prism[24-26].

1.2.4. Plaque Reduction Neutralization Test (PRNT)

The antiviral efficacy of NP4, NP5, and quercetin against DENV-2 was determined by PRNT as adapted from Cheng et al. (2002) and Jayasekara et al. (2024)[25,27]. Cells seeded at 2 × 10^5 cells/ml were pre-treated with varying concentrations of the compounds. After pretreatment, compound solutions were removed, cells were washed with PBS, and infected with DENV-2 suspension containing approximately 90–100 PFU/well. Virus adsorption was allowed for 1 hour at 37°C, followed by overlaying cells with medium containing 1% methylcellulose or carboxymethyl cellulose to restrict viral spread. After a 5-day incubation, the cells were fixed with 10% formalin, followed by staining with 1% crystal violet. Plaques were counted manually, and percentage plaque inhibition compared to virus controls was calculated. The IC_{50} (compound concentration achieving 50% plaque reduction) was calculated by nonlinear regression using GraphPad Prism[25-27].

1.2.5. *In vitro* Cytopathic Effect (CPE)-based Antiviral Assay

The antiviral potential of phytocompounds was evaluated using a CPE-based *in vitro* antiviral assay. Vero E6 cells were seeded into 96-well plates at a density of 1.5 × 10^4 cells/well and incubated at 37°C with 5% CO_2 for 24 hours. After virus adsorption, inoculum was removed, and cells were washed with serum-free medium. The test compounds were added at their predetermined MNTD concentrations (based on MTT assay results) to the respective wells. The plate was further incubated for 5 days, with daily microscopic evaluation of CPE. The degree of viral inhibition was assessed using the standard grading scale described as : '++++' = complete inhibition of CPE, '+++' = 75% inhibition, '++' = 50% inhibition, '+' = <50% inhibition, '–' = no inhibition. Each experimental condition was tested in triplicates[24,25,27,28].

To validate the antiviral effect observed microscopically, MTT assays were performed in parallel to quantify cell viability. Cells from the above treatment groups (cells alone, DENV-infected cells, and infected cells treated with test compounds) were incubated with MTT reagent for 3 hours. The resulting formazan crystals were dissolved in DMSO, and absorbance was measured at 570 nm using a microplate reader. The percentage cell viability was calculated, and results were statistically compared to the virus control group using an unpaired Student's t-test. Results were expressed as mean ± SD. Differences were considered statistically significant at $p < 0.05$. All statistical analyses were performed using GraphPad Prism[24,28].

RESULTS and DISCUSSION

1.3. HTVS Analysis

A graphical representation of the docking scores obtained from HTVS is given in **figure 2**. The compounds were filtered considering -8 kcal/mol as the cut off value and the intermolecular interactions of these complexes were examined. The compounds were then filtered again based on receptor-ligand binding complementarity, standard inhibitors and the compounds that are the subject of ongoing study/trials. Upon thorough analysis, the best five hit compounds were considered for further analysis.

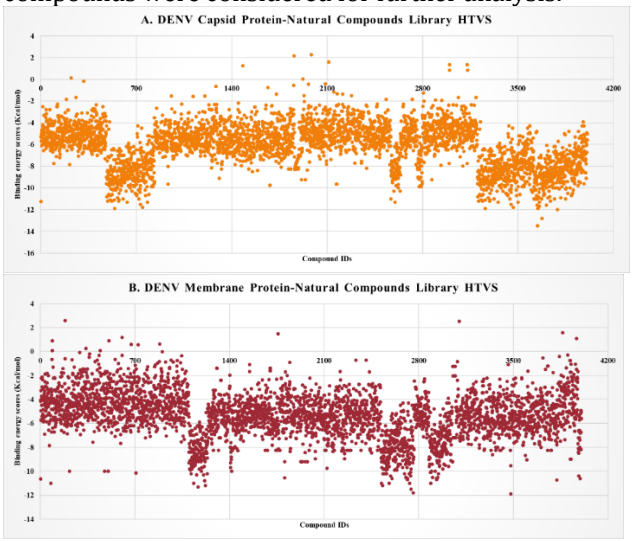

© 2025 European Journal of Clinical Pharmacy; All Right Reserved

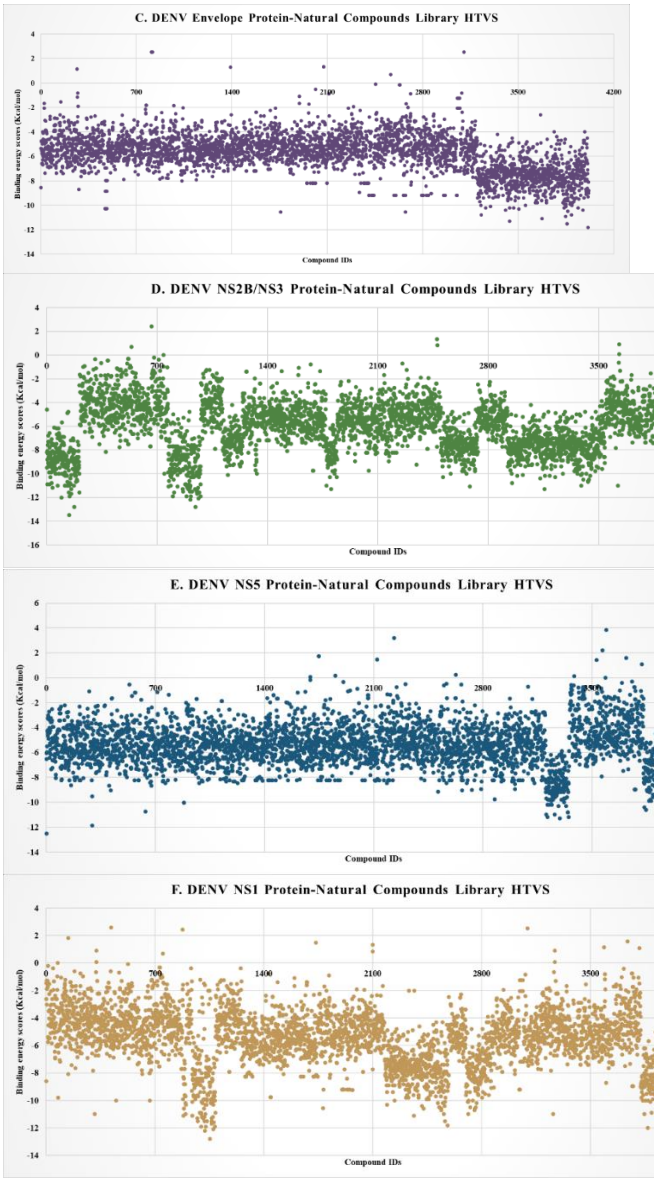

Figure 2. A graphical representation of the docking scores (Kcal/mol) of the ligands docked to A. capsid protein are represented in orange, B. membrane protein in red, C. envelope protein in purple, D. NS2B/NS3 protein in green, E. NS5 protein in blue and F. NS1 protein in brown.

1.4. Specific Molecular Docking Analysis

The docking scores of the top hits labelled as NP1-NP5 docked to respective proteins are represented in **figure 3**. **Table 2** summarizes the molecular docking details of these docked complexes.

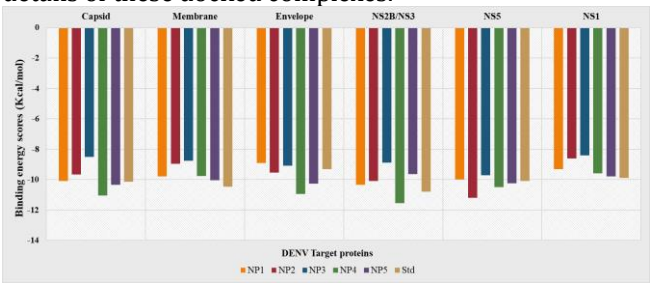

Figure 3. A graphical representation of the binding energy scores of the top five NP hits bound to the target proteins. Each bar of the graph represents colour coded compounds.

Ligands that bind firmly to target proteins are selected as lead compounds. Interactions include hydrophobic contacts, hydrogen bonds, π-stacking, salt bridges, amide stacking, and cation–π interactions. The ligand interaction diagram shows different coloured binding site residues of the proteins (**Figure 4 (A-F)**).

Table 2. Specific molecular docking details of the compounds, NP1-NP5, relative to a standard antiviral DENV compound.

Sl. No.	Target Protein	Compound ID	Docking Score (kcal/mol)	Hydrogen Bonds	Other Interactions
1	Capsid premembrane protein	NP1	-10.1	2	-
		NP2	-9.67	1	-
		NP3	-8.5	0	-
		NP4	-11.04	1	-
		NP5	-10.33	4	-
		Standard	-11.01	2	-
2	Small membrane protein M	NP1	-9.8	3	1 salt bridge, 2 pi-cation
		NP2	-8.76	1	1 salt bridge, 1 pi-cation
		NP3	-9.76	0	-
		NP4	-10.04	2	1 salt bridge, 1 pi-pi stacking, 2 pi-cation

© 2025 European Journal of Clinical Pharmacy; All Right Reserved

		NP5	-10.47	4	1 salt bridge, 1 pi-pi stacking
		Standard	-11.01	1	1 salt bridge
3	Major envelope protein E	NP1	-8.91	2	2 pi-pi stacking
		NP2	-9.54	5	-
		NP3	-9.09	0	1 salt bridge
		NP4	-10.95	3	1 salt bridge
		NP5	-10.27	4	1 salt bridge
		Standard	-9.32	6	-
4	NS2B/NS3 Protease	NP1	-10.3	3	1 salt bridge
		NP2	-10.1	4	-
		NP3	-8.89	0	1 salt bridge
		NP4	-11.56	2	1 salt bridge, 1 pi-cation
		NP5	-9.8	4	1 salt bridge
		Standard	-10.8	3	1 salt bridge
5	NS5 protein	NP1	-9.98	3	2 pi-cation
		NP2	-11.2	5	1 salt bridge
		NP3	-9.71	1	2 pi-cation, 2 pi-pi stacking
		NP4	-10.5	1	2 salt bridge
		NP5	-10.23	4	1 salt bridge
		Standard	-10.1	2	1 salt bridge, 1 pi-pi stacking
6	NS1 protein	NP1	-9.3	1	1 pi-cation, 1 pi-pi Stacking
		NP2	-8.6	2	1 salt bridge
		NP3	-8.4	0	1 salt bridge
		NP4	-9.6	2	1 salt bridge, 1 pi-pi Stacking
		NP5	-9.8	6	2 pi-cation, 1 pi-pi Stacking
		Standard	-9.9	3	2 salt bridge, 1 pi-cation

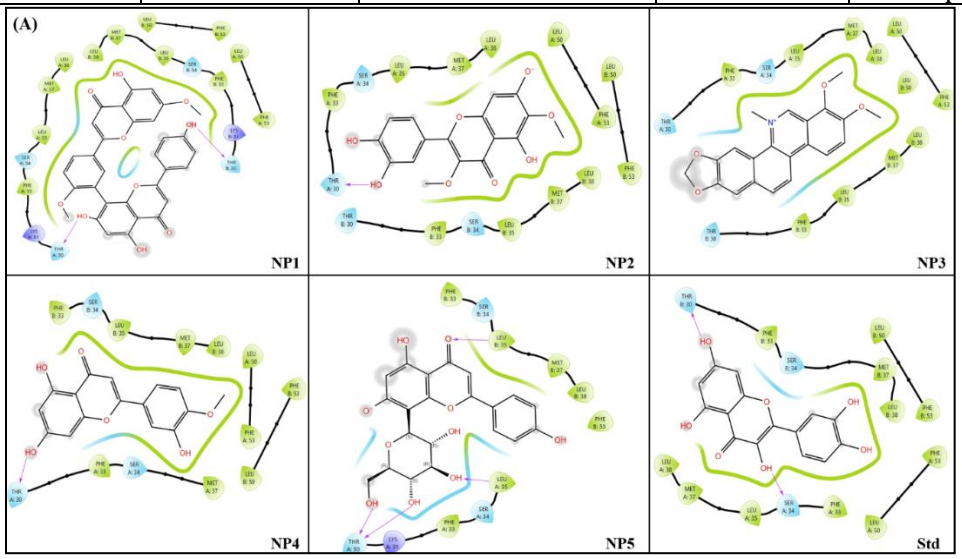

© 2025 European Journal of Clinical Pharmacy; All Right Reserved

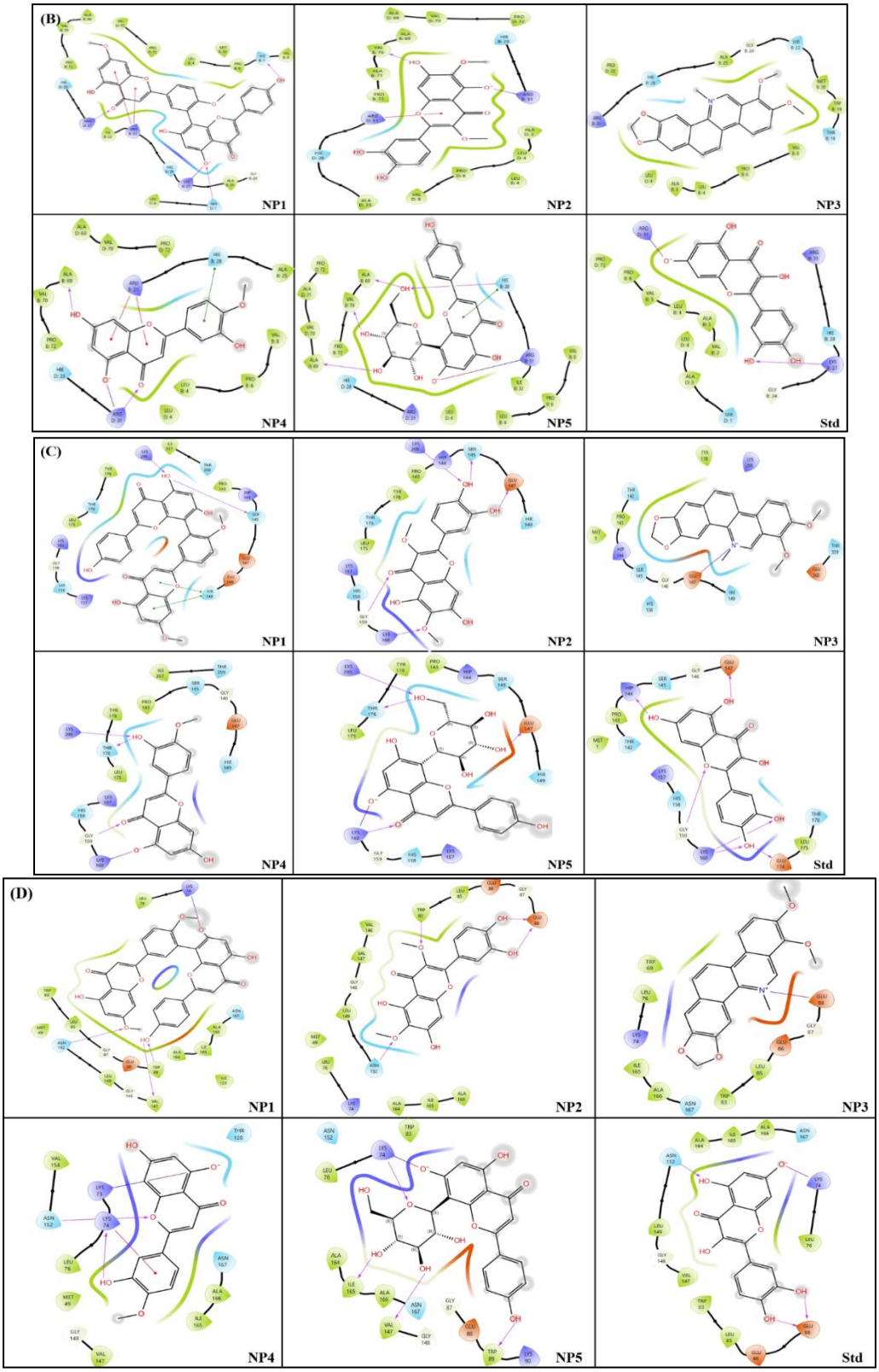

 © 2025 European Journal of Clinical Pharmacy; All Right Reserved

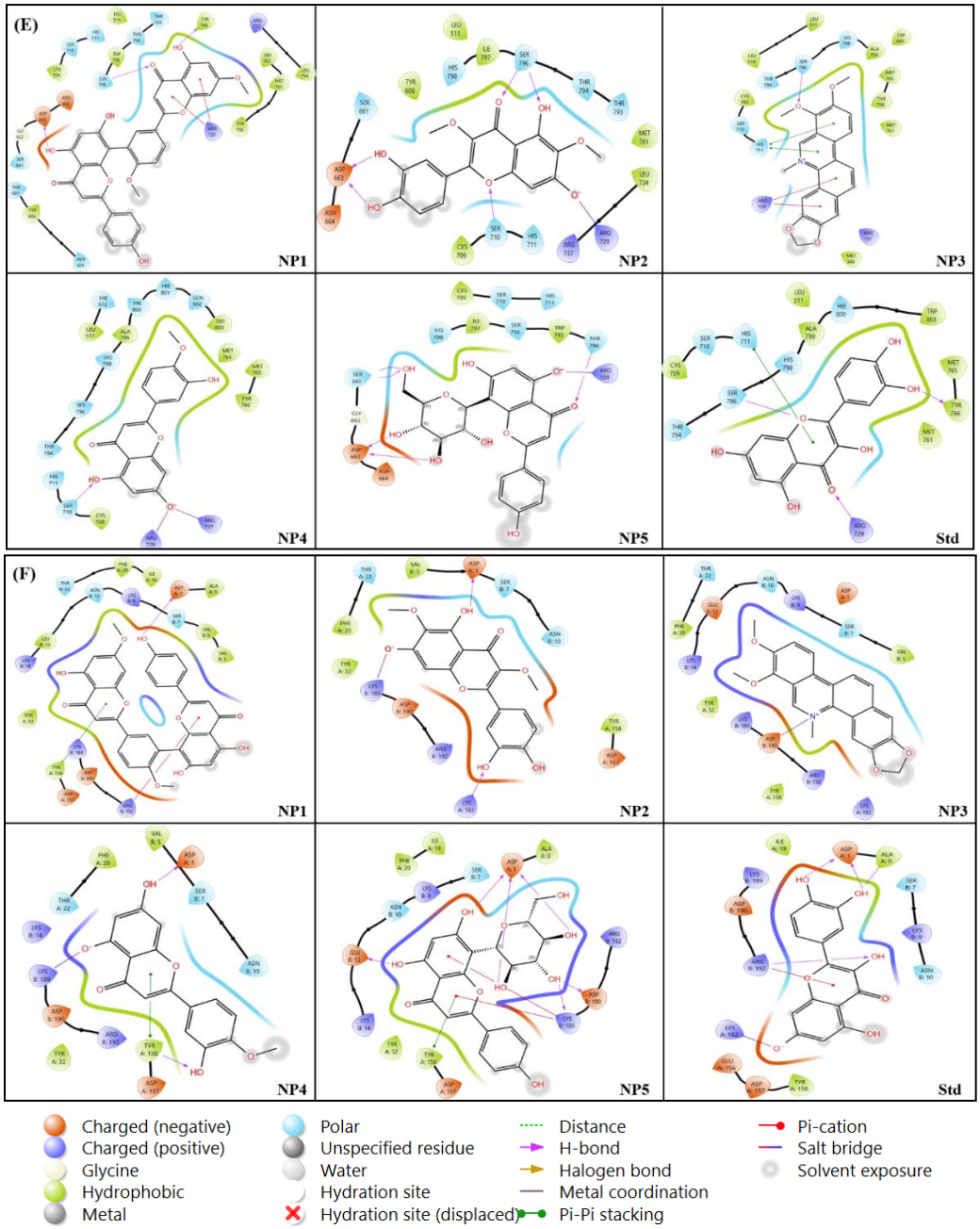

Figure 4. Two-dimensional protein-ligand interactions of compounds, NP1-NP5 bound to the DENV proteins in comparison with the standard inhibitor. Green coloured discs represent hydrophobic residues, cyan denotes polar residue, blue is positively charged residue and red is negatively charged. The grey coloured atom background denotes per-atom solvent accessible surface area (SASA).

Based on the above data, for the capsid protein, NP4 exhibited the strongest binding affinity, outperforming the standard, while NP5 formed 4 hydrogen bonds, suggesting a more stable interaction. For the membrane protein, NP5 emerged as the top-scoring phytocompound, forming 4 H-bonds and interacting via 1 salt bridge and 1 π-π stacking. NP4 also showed strong binding (-10.04 kcal/mol) with rich interactions including 1 salt bridge, 1 π-π stacking, and 2 π-cation bonds. Both compounds approached the standard score (-11.01 kcal/mol), indicating significant inhibitory potential. For the envelope protein, NP4 showed the least affinity while NP5 shared 5 H-bonds and a salt bridge, indicating these two compounds could effectively disrupt envelope protein-mediated viral entry. For NS2B/NS3 Protease, NP4 was the most favourable compound, better than the standard. For the NS5 protein, although NP2 had the highest score, NP4 showed s strong docking affinity with 2 salt bridges and NP5 showed 4 H-bonds indicating effective target

© 2025 European Journal of Clinical Pharmacy; All Right Reserved

engagement. NP5 demonstrated excellent binding, forming the highest number of hydrogen bonds along with 2 π-cation and 1 π-π stacking interactions, closely matching the standard (–9.9 kcal/mol). NP4 also showed favourable results with 2 hydrogen bonds, 1 salt bridge, and 1 π-π stacking, supporting their potential in targeting NS1-associated immune evasion. Across all six dengue virus targets, NP4 and NP5 consistently showed high docking scores and key molecular interactions, sometimes outperforming the standard drug. Their multi-target potential highlights them as lead candidates for further anlaysis and *in vitro* antiviral assays.

1.5. MM/GBSA Analysis

A greater negative value denotes stronger binding as the MM-GBSA binding energies are approximations of the free energies of binding. It was also possible to determine the importance of the dGBind Coulomb (Coulomb energy), dGBind Hbond (Hydrogen bonding correction), dGBind Lipo (Lipophilicity energy), and dGBind vdW (Van der Waals energy). The information of the top hit compounds considered for further analysis is summarized in **table 3**.

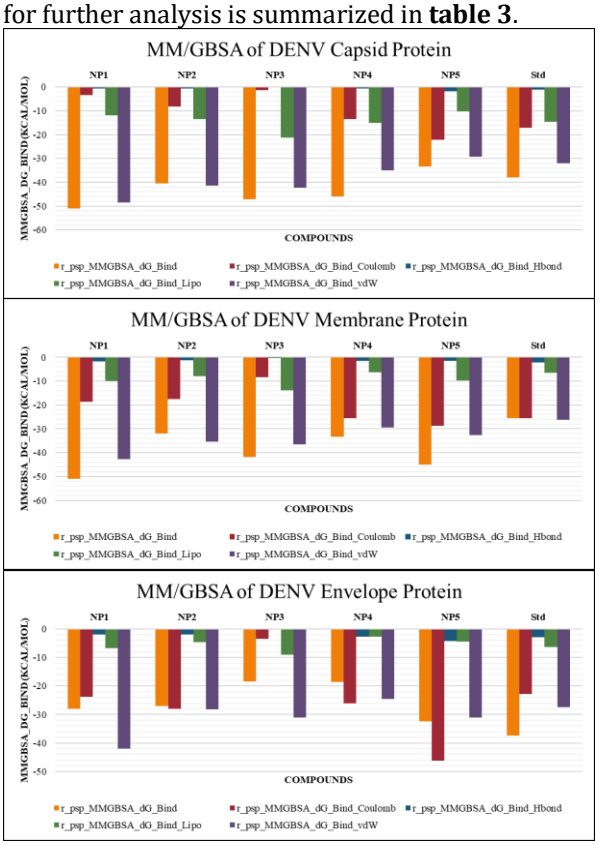

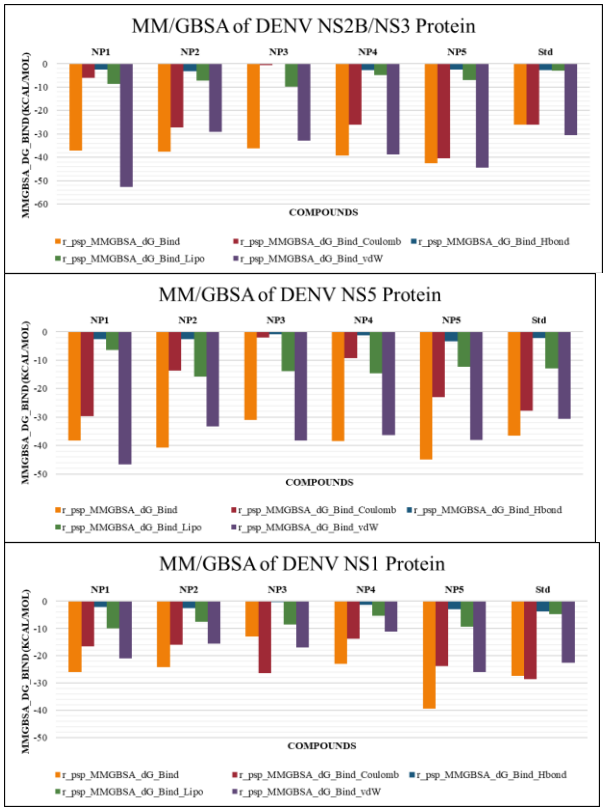

Figure 5. Assessment of the binding free energy (orange bars) and other relative free energies (kcal/mol) such as coulomb energy (red), hydrogen bonding energy (dark blue), lipophilicity energy (dark green) and Van der Waals energy (dark purple) obtained by Prime MM-GBSA for the complexes of DENV target proteins to NP1-NP5 in comparison with the standard.

The MM/GBSA binding free energy analysis across six key dengue virus proteins revealed that compounds NP4 and NP5 consistently exhibited the most favourable binding affinities (Figure 5). Their interactions were predominantly stabilized by the other interactions, indicating strong and specific binding within the active sites of the viral proteins

Table 3. Information of the top Natural compounds screened for further inter-molecular interactions.

Compound ID	Compound Name	PubChem ID	Drug Class	Structure
NP1	Ginkgetin	5271805	Biflavonoid	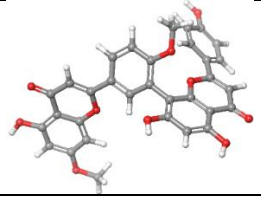

© 2025 European Journal of Clinical Pharmacy; All Right Reserved

NP2	Axillarin	5281603	Flavonol glycoside	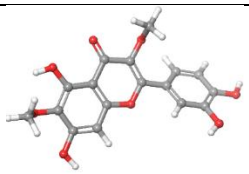
NP3	Chelerythrine	2703	Benzophenanthridine alkaloid	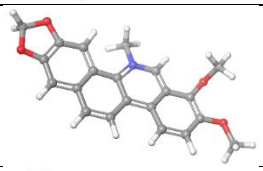
NP4	Diosmetin	5281612	Flavone (O-methylated)	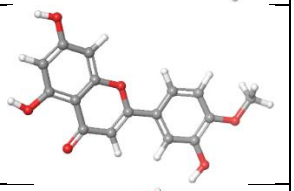
NP5	Vitexin	5280441	Flavone C-glycoside	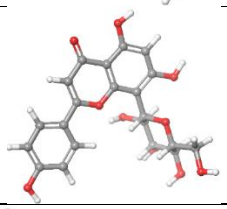
Standard	Quercetin	5280343	Flavonol	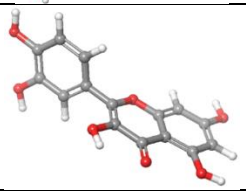

1.6. Molecular Dynamics Simulation (MDS) Analyses

The two best compounds were further considered to determine the stability of the docked complex. **Figure 6** represents the simulation box built to run MDS.

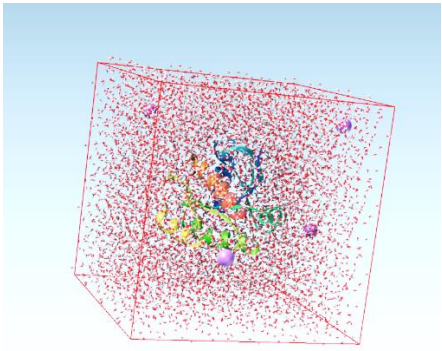

Figure 6. MD simulation box surrounding the simulation system of a docked complex comprising of ions to neutralize the system and water solvent molecules.

Using ligand root mean square deviation (RMSD), we were able to deduce the stability of the ligand with respect to the protein as well as the shift in the ligand's internal conformation (**Figure 7**). Larger alterations suggested that the protein had gone through a significant conformational shift during the simulation. The trajectories were analysed using simulation interaction diagram of Desmond module and the graphs were combined to a single frame using qtgrace v026 software.

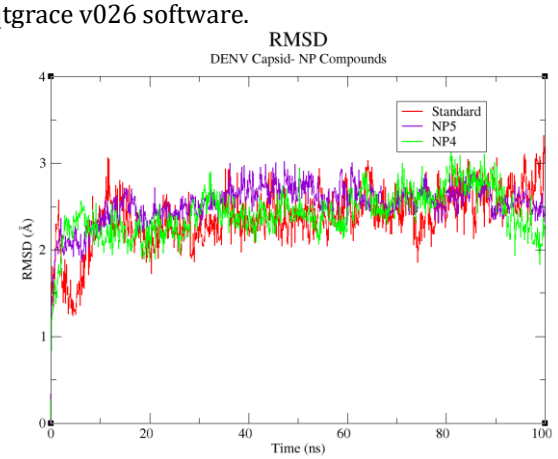

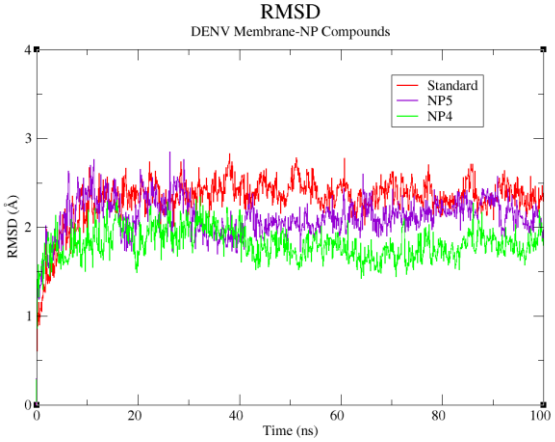

© 2025 European Journal of Clinical Pharmacy; All Right Reserved

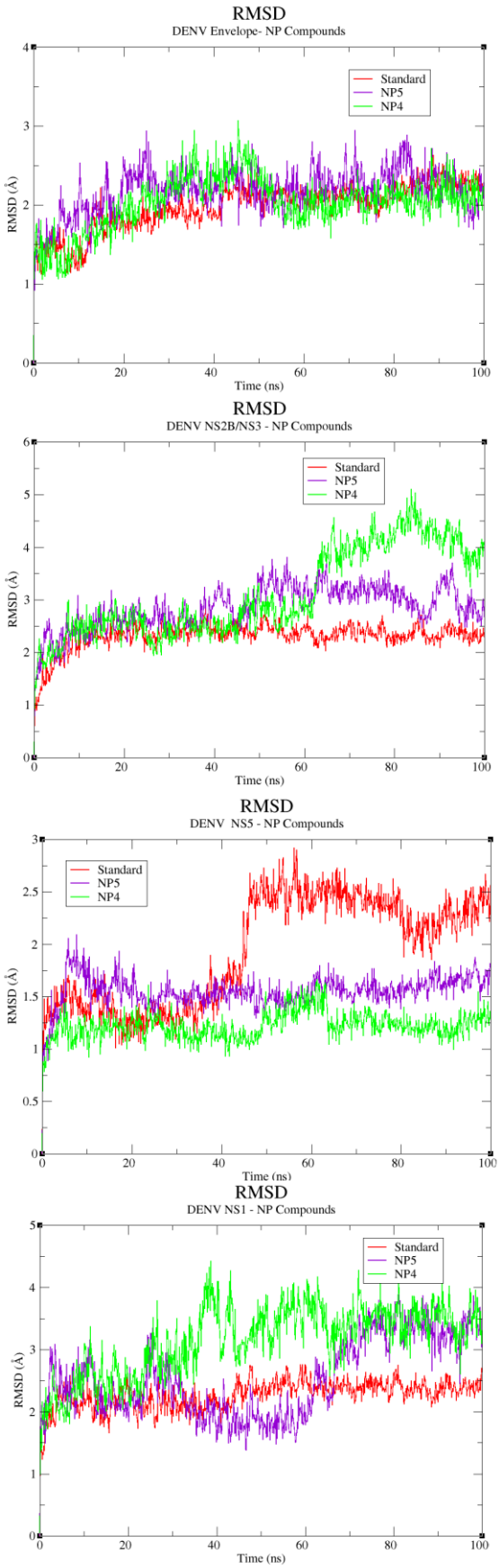

Figure 7. RMSD analysis of DENV proteins docked with NP5 (indigo coloured) and NP4 (green coloured) in comparison with the standard (red coloured).

Using the desmond module, 100ns run was performed on these docked complexes to get better insights in the complex stability.

Based on figure 6, for the DENV Capsid protein, NP4 and NP5 complexes showed consistent RMSD fluctuations between ~2.0 to 3.0 Å, which is comparable to the standard compound, indicating that the binding was generally stable during the simulation. All three ligands (NP4, NP5, and standard) exhibited a similar RMSD trend for the envelope protein, varying between ~1.5 and 2.5 Å. NP5 showed better stability than NP4 for NS2B/NS3 protease, with RMSD below 3.5 Å. In contrast, NP4 had significantly higher fluctuations (>4 Å after 60 ns), indicating a less stable interaction. For NS5 protein, compared to NP5 and standard, NP4 exhibited the most stable RMSD trajectory (~1.2-1.5 Å). For NS1 protein, NP4 again showed larger fluctuations (~4.0-4.5 Å), while NP5 exhibited relatively better stability (~2.5-3.5 Å). The standard compound remained the most stable with RMSD around ~2.0-2.3 Å. Based on the computational analyses, compounds NP4 and NP5 were considered for further *in vitro* assays to evaluate the antiviral property.

1.7. ROS scavenging activity

The results demonstrate the antioxidant and cytoprotective effects of the test compounds on HEPG2 cells. Flow cytometry analysis revealed that the control group exhibited baseline ROS levels, with 18.6% of cells showing DCF fluorescence, representing normal physiological conditions. In contrast, the H_2O_2-treated group displayed a significant increase in ROS levels, with 40.4% of cells showing fluorescence, indicating severe oxidative stress, which can disrupt mitochondrial function and induce cell death. Similarly, NP5 reduced ROS levels to 28.0%, though its effect was slightly less potent than that of NP4 at its IC_{50} concentration. Both the compounds showed significant antioxidant activity compared to the H_2O_2 group, indicating their ability to mitigate oxidative stress and protect cells from ROS-induced damage. These findings highlight the potential of both plant extracts, particularly NP5 as natural antioxidants capable of restoring redox balance and protecting cells from oxidative stress *in vitro* shown in below **Figure 8**.

© 2025 European Journal of Clinical Pharmacy; All Right Reserved

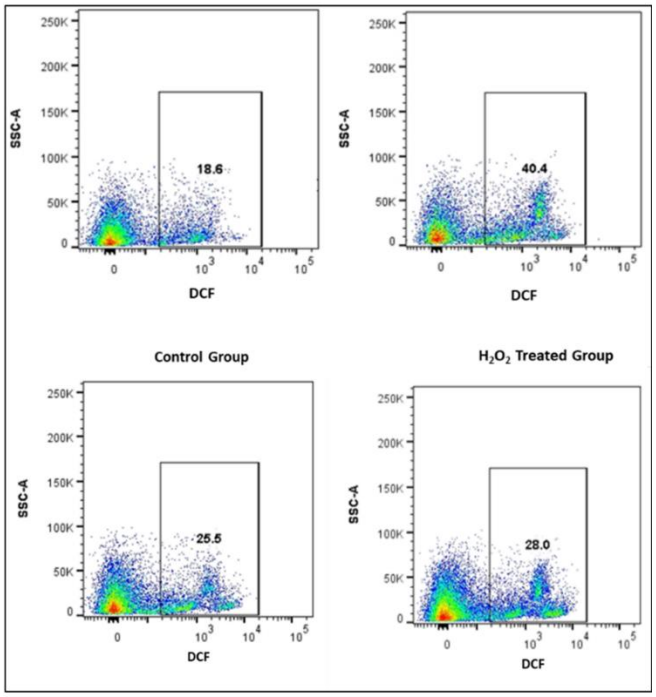

Figure 8. Flow-cytometry-based assay of ROS levels cells after different treatments. Statistical significance compared with the H_2O_2 group is shown (****p < 0.0001; ***p < 0.001).

1.8. Cytotoxicity Assay (MTT) of the lead compounds

As shown in **figure 9**, the compounds exhibited a concentration-dependent reduction in cell viability. Among the tested compounds, NP5 exhibited the highest CC_{50} value (87.2 µg/mL), indicating lower cytotoxicity, followed by NP4 (CC_{50} = 74.6 µg/mL) and quercetin (CC_{50} = 82.5 µg/mL). The corresponding $MNTD_{80}$ values were also highest for NP5 (62.5 µg/mL), followed by quercetin (55.3 µg/mL) and NP4 (48.1 µg/mL), suggesting their suitability for further antiviral assays. The values fall within the acceptable cytotoxicity limits reported for medicinal plant compounds in *in vitro* systems.

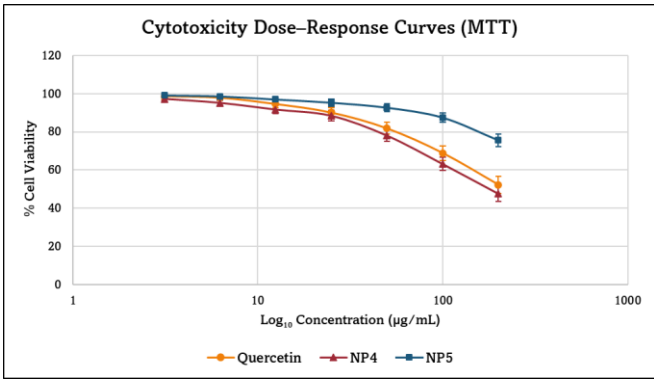

Figure 9. Dose–response curves depicting the cytotoxic effects of NP4, NP5, and quercetin on Vero cells after 48 hours of treatment. Cell viability (% of untreated control) was measured using the MTT assay across a range of compound concentrations (3.13–200 µg/mL) plotted on a logarithmic scale. Each data point represents mean ± standard deviation of triplicates.

1.9. Plaque Reduction Neutralization Test (PRNT)

Quercetin demonstrated an IC_{50} of 9.8 µg/mL, consistent with its known antiviral activity. NP4 showed moderate plaque reduction with an IC_{50} of 13.4 µg/mL, whereas NP5 showed the most potent activity with an IC_{50} of 6.3 µg/mL, indicating superior efficacy compared to quercetin. The percentage of plaque inhibition was 86.9 ± 1.8, 65.2 ± 3.0 and 78.6 ± 2.4 for NP5, NP4, and quercetin, respectively, highlighting NP5 as the most potent inhibitor among the tested phytocompounds (**Figure 10**).

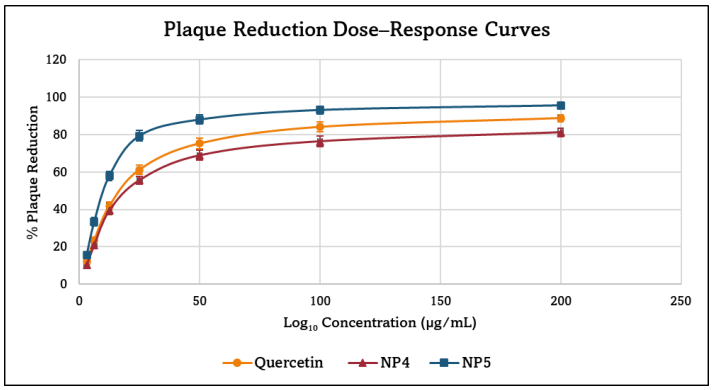

Figure 10. Dose-dependent plaque reduction curves for NP4, NP5, and quercetin against DENV in Vero cells, as determined by the plaque reduction neutralization test (PRNT). Percent plaque inhibition was quantified relative to virus control following 5-day infection across increasing compound concentrations (3.13–200 µg/mL, logarithmic scale). Each data point represents mean ± standard deviation of triplicates.

1.10. *In vitro* Antiviral Assay

The antiviral efficacy of NP4, NP5, and quercetin at their respective $MNTD_{80}$ was evaluated using a CPE inhibition assay in Vero E6 cells. Microscopic evaluation showed that NP5 achieved near-complete inhibition of CPE ('+++ to ++++'), while NP4 showed moderate protection ('++'). Quercetin showed strong inhibition ('+++') as expected.

These results were validated by parallel MTT assays. Untreated virus-infected wells showed a viability of 24 ± 3.0%, indicating high viral cytotoxicity. Quercetin treatment improved viability to 76 ± 4.0%, while NP4 and NP5 increased viability to 72 ± 3.8% and 78 ± 3.6%, respectively ($p < 0.05$). The heightened viability in NP5-treated groups reinforces its superior antiviral activity (**Figure 11**).

© 2025 European Journal of Clinical Pharmacy; All Right Reserved

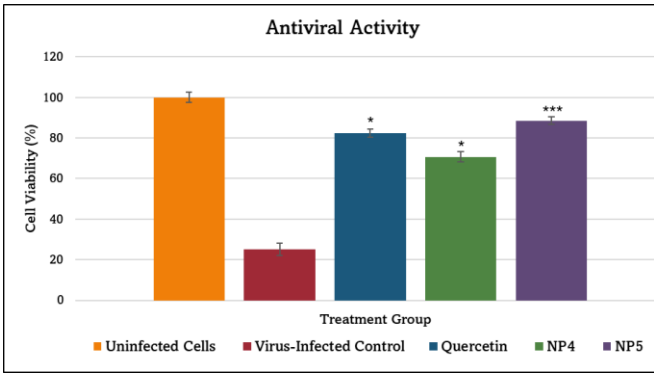

Figure 11. Bar graph depicting cytopathic effect (CPE) inhibition grading and corresponding Vero cell viability (%) upon treatment with NP4, NP5, and quercetin at their respective $MNTD_{80}$ concentrations following DENV-2 infection. Cell viability measured by MTT assay (mean ± SD, n=3). Statistical significance compared to virus-infected control was determined via one-way ANOVA with Tukey's multiple comparison test. Significance levels: $p < 0.05$ (*), $p < 0.01$ (**), $p < 0.001$ (***).

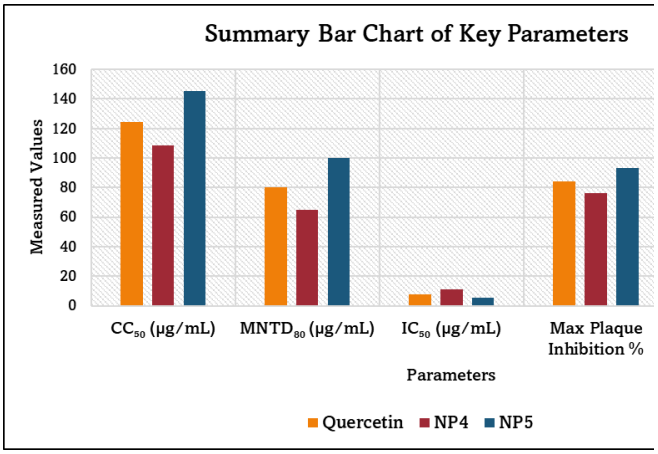

Figure 12. Comparative bar chart summarizing major efficacy and cytotoxicity parameters for NP4, NP5, and quercetin: CC_{50} (50% cytotoxic concentration), $MNTD_{80}$ (maximum non-toxic dose at ≥80% viability), IC_{50} (50% inhibitory concentration for plaque reduction), maximum percent plaque inhibition, and percent cell viability at $MNTD_{80}$.

The comparative analysis of NP4, NP5, and the standard quercetin demonstrates distinct safety and antiviral efficacy profiles (**Figure 12**). The higher CC_{50} and $MNTD_{80}$ for NP5 indicate that it is less cytotoxic and can be used at higher working concentrations, expanding its therapeutic window for antiviral activity. The lower IC_{50} and higher percentage of plaque inhibition for NP5 highlight its potent inhibitory effects at lower doses compared to both NP4 and quercetin. The observed levels of cell viability and visual CPE inhibition suggest NP5 efficiently suppresses DENV-2 replication and preserves host cell integrity even at higher viral titers.

In conclusion, the integrated data from cytotoxicity, plaque reduction, and *in vitro* antiviral tests collectively demonstrate that NP5 outperforms both NP4 and quercetin, emerging as a highly promising lead compound for future anti-dengue interventions.

CONCLUSION

In this study, we successfully integrated computational drug discovery with *in vitro* biological assays to identify potential anti-dengue compounds from a library of natural products. High-throughput virtual screening and MM/GBSA analysis identified five lead phytocompounds (NP1–NP5) with exceptional binding affinities across six critical DENV target proteins. MD simulations further confirmed the stability of these protein-ligand complexes, suggesting a robust mechanism of action.

Significant anti-dengue potential was shown by the experimental validation of the top-performing hits, namely Diosmetin and Vitexin. NP4 (Diosmetin) and NP5 (Vitexin), the principal chemicals found, are well-known natural flavonoids with proven medicinal uses. Diosmetin, which has long been known to be found in citrus fruits and used to treat inflammation and venous insufficiency, showed high binding to several DENV proteins. Similarly, the most effective option in our investigation was vitexin, a substance with cardioprotective, anti-inflammatory, and antioxidant qualities that is present in hawthorn and passionflower.

Significant anti-dengue potential was shown by the experimental validation of these hits, with Vitexin in particular demonstrating higher efficacy in CPE-based assays and PRNT. Additionally, these compounds' ability to scavenge ROS points to a potential additional therapeutic effect in reducing the oxidative stress commonly linked to DENV infection. These results support the prioritization of NP5 for deeper mechanistic studies (e.g., entry inhibition, viral RNA synthesis blockage), *in vivo* efficacy models, and safety pharmacology assessments. Importantly, these outcomes align closely with profiles reported for established and experimental antivirals in the literature, underscoring the scientific credibility of NP5's antiviral potential. When combined, our results show that these phytocompounds are attractive scaffolds for the development of multi-target dengue treatments, utilizing their current pharmacological characteristics to hasten the development of new medications. Future prospects involve the structural optimization of these leads to enhance bioavailability and the initiation of *in vivo* studies to evaluate their protective efficacy in lethal DENV challenge models.

CONFLICT OF INTEREST

The authors declare that the research was conducted in the absence of any commercial or financial relationships that could be construed as a potential conflict of interest.

© 2025 European Journal of Clinical Pharmacy; All Right Reserved

AUTHOR CONTRIBUTIONS

Conceptualization, T.S.D., G.S.M. and A.J.; methodology, A.J, B.S. and C.D. ; validation and formal analysis, C.S., C.S., and G.S.M.; data curation, C.D., A.J., and B.S,; writing-original draft preparation, A.J., C.S., C.D., B.S. and C.S.; writing-review and editing, C.S., C.S., G.S.M. All authors have read and agreed to the published version of the manuscript.

REFERENCES:

1. World Health Organization. (2025, April 30). Dengue and severe dengue. https://www.who.int/news-room/fact-sheets/detail/dengue-and-severe-dengue
2. Roy, S. K., & Bhattacharjee, S. (2021). Dengue virus: Epidemiology, biology, and disease aetiology. Canadian Journal of Microbiology, 67(10), 687–702. https://doi.org/10.1139/cjm-2020-0572
3. World Health Organization. (2025, April 24). Global dengue surveillance. https://worldhealthorg.shinyapps.io/dengue_global/
4. Journal of Infectious Diseases and Epidemiology. (n.d.). Article on dengue. https://clinmedjournals.org/articles/jide/journal-of-infectious-diseases-and-epidemiology-jide-2-015.php
5. World Health Organization. (2019). Ten threats to global health in 2019. https://www.who.int/news-room/spotlight/ten-threats-to-global-health-in-2019
6. Nanaware, N., Banerjee, A., Mullick Bagchi, S., Bagchi, P., & Mukherjee, A. (2021). Dengue virus infection: A tale of viral exploitations and host responses. Viruses, 13(10), 1967. https://doi.org/10.3390/v13101967
7. Lim, S. Y. M., Chieng, J. Y., & Pan, Y. (2020). Recent insights on anti-dengue virus (DENV) medicinal plants: Review on in vitro, in vivo and in silico discoveries. All Life, 14(1), 1–33. https://doi.org/10.1080/26895293.2020.1856192
8. Saleh, M. S. M., & Kamisah, Y. (2021). Potential medicinal plants for the treatment of dengue fever and severe acute respiratory syndrome–coronavirus. Biomolecules, 11(1), 42. https://doi.org/10.3390/biom11010042
9. Haq, A., Mallawarachchi, S., Anderson, A., Khaleghi, L., Manujitha, L., & Fernando, S. (2025). In silico evaluation of potential hit molecules against multiple serotypes of dengue virus envelope glycoprotein. Molecules, 30(6), 1268. https://doi.org/10.3390/molecules30061268
10. Berman, H. M., Westbrook, J., Feng, Z., Gilliland, G., Bhat, T. N., Weissig, H., Shindyalov, I. N., & Bourne, P. E. (2000). The Protein Data Bank. Nucleic Acids Research, 28(1), 235–242
11. Xia, H., Xie, X., Zou, J., Noble, C. G., Russell, W. K., Holthauzen, L. M. F., Choi, K. H., White, M. A., & Shi, P. Y. (2020). A cocrystal structure of dengue capsid protein in complex with an inhibitor. Proceedings of the National Academy of Sciences of the United States of America, 117(30), 17992–18001. https://doi.org/10.1073/pnas.2003056117
12. Erbel, P., Schiering, N., D'Arcy, A., Renatus, M., Kroemer, M., Lim, S. P., Yin, Z., Keller, T. H., Vasudevan, S. G., & Hommel, U. (2006). Structural basis for the activation of flaviviral NS3 proteases from dengue and West Nile virus. Nature Structural & Molecular Biology, 13, 372–373. https://doi.org/10.1038/nsmb1073
13. Zhang, X., Ge, P., Yu, X., Brannan, J. M., Bi, G., Zhang, Q., Schein, S., & Zhou, Z. H. (2013). Cryo-EM structure of the mature dengue virus at 3.5-Å resolution. Nature Structural & Molecular Biology, 20, 105–110. https://doi.org/10.1038/nsmb.2463
14. Lim, S. P., Noble, C. G., Seh, C. C., Soh, T. S., El Sahili, A., Chan, G. K., Lescar, J., Arora, R., Benson, T., Nilar, S., & Shi, P. Y. (2016). Potent allosteric dengue virus NS5 polymerase inhibitors: Mechanism of action and resistance profiling. PLOS Pathogens, 12(8), e1005737. https://doi.org/10.1371/journal.ppat.1005737
15. Akey, D. L., Brown, W. C., Konwerski, J. R., Jose, J., DelProposto, J., Ogata, C. M., Skiniotis, G., Kuhn, R. J., & Smith, J. L. (2014). Flavivirus NS1 structures reveal surfaces for associations with membranes and the immune system. Science, 343(6173), 881–885. https://doi.org/10.1126/science.1247749
16. Fu, L., Ye, F., Feng, Y., Yu, F., Wang, Q., Wu, Y., Zhao, C., Sun, H., Huang, B., Niu, P., Song, H., Shi, Y., Li, X., Tan, W., Qi, J., Gao, G. F., & Gao, J. (2020). Both boceprevir and GC376 efficaciously inhibit SARS-CoV-2 by targeting its main protease. Nature Communications, 11(1), 4417. https://doi.org/10.1038/s41467-020-18233-x
17. Lans, C., & van Asseldonk, T. (2020). Dr. Duke's phytochemical and ethnobotanical databases, a cornerstone in the validation of ethnoveterinary medicinal plants. In Á. Máthé (Ed.), Medicinal and aromatic plants of North America (Vol. 6). Springer. https://doi.org/10.1007/978-3-030-44930-8_10
18. Jain, A. S., Sushma, P., Dharmashekar, C., Beelagi, M. S., Prasad, S. K., Shivamallu, C., & Prasad, A. (2021). In silico evaluation of flavonoids as effective antiviral agents on the spike glycoprotein of SARS-CoV-2. Saudi Journal of Biological Sciences, 28(1), 1040–1051.
19. Purohit, P., Barik, D., Agasti, S., Panda, M., & Meher, B. R. (2024). Evaluation of the inhibitory potency of anti-dengue phytocompounds against DENV-2 NS2B-NS3 protease: Virtual screening, ADMET profiling and molecular dynamics simulation

 © 2025 European Journal of Clinical Pharmacy; All Right Reserved

investigations. Journal of Biomolecular Structure and Dynamics, 42(6), 2990–3009.

20. Shin, H. J., Kim, M. H., Lee, J. Y., Hwang, I., Yoon, G. Y., Kim, H. S., Kwon, Y. C., Ahn, D. G., Kim, K. D., Kim, B. T., et al. (2021). Structure-based virtual screening: Identification of a novel NS2B-NS3 protease inhibitor with potent antiviral activity against Zika and dengue viruses. Microorganisms, 9, 545. https://doi.org/10.3390/microorganisms9030545
21. Tsakni, A., Kyriakopoulou, E., Letsiou, S., Halvatsiotis, P., Rigopoulos, H., Vassilaki, N., & Houhoula, D. (2025). In vitro determination of antimicrobial, antioxidant and antiviral properties of Greek plant extracts. Microorganisms, 13, 177. https://doi.org/10.3390/microorganisms13010177
22. Altamish, M., Khan, M., Baig, M. S., Pathak, B., Rani, V., Akhtar, J., Khan, A. A., Ahmad, S., & Krishnan, A. (2022). Therapeutic potential of medicinal plants against dengue infection: A mechanistic viewpoint. ACS Omega, 7(28), 24048–24065. https://doi.org/10.1021/acsomega.2c00625
23. Low, Z. X., OuYong, B. M., Hassandarvish, P., Poh, C. L., & Ramanathan, B. (2021). Antiviral activity of silymarin and baicalein against dengue virus. Scientific Reports, 11(1), 21221. https://doi.org/10.1038/s41598-021-98949-y
24. Tang, L. I., Ling, A. P., Koh, R. Y., Chye, S. M., & Voon, K. G. (2012). Screening of anti-dengue activity in methanolic extracts of medicinal plants. BMC Complementary and Alternative Medicine, 12, 3. https://doi.org/10.1186/1472-6882-12-3
25. Jayasekara, K. G., Suresh, S., Goonasekara, C., Wijesundara, N. M., & Wijewardana, V. (2024). Anti-dengue viral activity of Glycyrrhiza glabra roots in Vero cells. Scientific Reports, 14, 25922. https://doi.org/10.1038/s41598-024-76184-5
26. Abdul Ahmad, S. A., Palanisamy, U. D., Tejo, B. A., Chew, M. F., Tham, H. W., & Syed Hassan, S. (2017). Geraniin extracted from the rind of Nephelium lappaceum binds to dengue virus type-2 envelope protein and inhibits early stage of virus replication. Virology Journal, 14(1), 229. https://doi.org/10.1186/s12985-017-0895-1
27. Cheng, H. Y., Lin, C. C., & Lin, T. C. (2002). Anti–herpes simplex virus activity of Terminalia arjuna bark. Antiviral Research, 55(3), 447–455.
28. Kudi, A. C., & Myint, S. H. (1999). Antiviral activity of some Nigerian medicinal plant extracts. Journal of Ethnopharmacology, 68(1–3), 289–294. https://doi.org/10.1016/S0378-8741(99)00049-5

 © 2025 European Journal of Clinical Pharmacy; All Right Reserved